Sonic excitation by means of ultrasound; an experimental illustration of acoustic radiation forces

Forum Acusticum 2011 - Aalborg - Denmark

Sonic excitation by means of ultrasound; an experimental illustration of acoustic radiation forces

N.Bert Roozen
NOVIC Noise and Vibration Control, Burg.Strijbosstraat 1, 5591EL Heeze, the Netherlands.
E-mail: bert@novic.nl

Pieter Nuij, Henk Nijmeijer
Eindhoven University of Technology, Den Dolech 2, 5612 AZ Eindhoven, the Netherlands.

Summary
Ultrasonic acoustic waves are known to induce a vibration of particles around an equilibrium position. However, for large acoustic amplitudes, due to non-linear acoustic effects, a rectified, net acoustic radiation force can occur. Experimental work is performed in which the non-linear behavior is exploited to generate a dynamic acoustic radiation force that is used to dynamically excite a small structure at sonic frequencies. The dynamic radiation forces are quantified experimentally in an inverse manner from the structural displacement of the structure being excited by acoustic radiation forces.

PACS no. 43.25.Qp, 43.40.Cw

1. Introduction

In the field of experimental dynamics, contactless excitation has obvious advantages as compared to excitation by means of mechanical contact. Exciting a structure mechanically, for instance by means of a shaker, influences the dynamics of the structure, or it is practically impossible, such as in the case of small devices (e.g. MEMS structures). Ways to excite a structure in a contactless manner are electrodynamically, electrostatically, optically, aerodynamically and acoustically. This paper focuses on the use of ultrasonic acoustic radiation forces to excite structures in the audible frequency range. The main goal is to quantify the radiation forces experimentally.

Ultrasonic radiation forces are known for a long time, dating back to publications of Lord Rayleigh [1]. It is a topic of non-linear acoustics. The physics involved are quite complex. In this paper we will not attempt to give a detailed explanation, but refer the reader to a critical and historical review on radiation force and radiation pressure by Chu and Apfel [2].

A well known application of the acoustic radiation force is to determine the sound intensity of an ultrasonic wave. The radiation force exerted by an ultrasonic wave impinging on an object provides a means to determine the intensity of the incident acoustic wave, usually in water. In this application the radiation force is a static force, generated by a steady ultrasonic wave.

Fatemi and Greenleaf [3] showed that it is also possible to create an alternating, dynamic acoustic radiation force by combining two ultrasonic sound waves of slightly different angular frequencies ω_1 and ω_2. Because of the non-linear nature of the acoustic radiation force, a radiation force will be created at the sum and difference frequencies. In the biomedical community it is used as an imaging technique [4].

Huber et al. [5] were the first to suggest the application of dynamic acoustic radiation forces in air for modal analysis of small MEMS structures. In [6] Huber et al. used an ultrasonic transducer in air to excite a micro-cantilever dynamically. Another application in air is described by Huber and Fatemi [7], who used a radiation force to bring a reed of a music instrument into vibration.

To our knowledge, an experimental quantification of dynamic acoustic radiation forces in air is lacking. In this paper an experimental method is presented for the quantification of dynamic acoustic radiation forces in air that exploits the resonant behavior of a mechanical structure. The radiation force is determined indirectly, by measuring the mechanical response of the resonant structure. A model of the mechanical structure is created, from which the acoustic radiation force with unknown amplitude can be quantified.

2. Acoustic radiation force

King [8] derived an analytical model for the rectified, net force acting on a small spherical rigid particle due to a plane stationary acoustic wave in an ideal fluid. It reads

$$F = \frac{5\pi}{6}\frac{\hat{p}^2}{\rho c^2}ka^3 \tag{1}$$

where F is the rectified, net acoustic radiation force in the direction of the wave propagation, $\hat{p}$ is the peak pressure amplitude of the incident acoustic wave, ρ is the fluid density, c is the speed of sound, $k = \omega/c$ is the acoustic wave number, and a is the sphere radius. King's theory, given in Eq. 1, is only valid for sphere radii much smaller compared to the acoustic wavelength ($ka < 0.14$). See also [9] and [10]. From Eq. 1 it can be seen that the radiation force is proportional to the acoustic pressure squared, which illustrates the non-linear behavior of the acoustic radiation force. It can also be seen that, for small spheres in an acoustic plane wave, the acoustic radiation force is proportional to the frequency omega of the acoustic wave and proportional to the sphere radius to the cube power.

In case of a stationary acoustic wave, we are dealing with a static force. However, by modulating the amplitude of the acoustic wave, an alternating dynamic acoustic radiation force can be created [3]. The purpose of this paper is to quantify the dynamic acoustic radiation force in which the resonant behavior of a small mechanical structure is exploited. In the next section the resonant mechanical structure is discussed, along with the development of a model for its dynamics.

3. Sphere-on-rod model

The small, resonant mechanical structure comprises a sphere with a radius of 0.5 mm and a rod with a radius of 0.2 mm and a length of approximately 15 mm. Both the sphere and the rod are made from steel. In addition also spheres with a radius of 0.75 mm, 1 mm and 1.5 mm are used. The spheres are glued to the end of a rod and the rod is fixed at its base, as shown in Fig. 1.

The resonance frequency of the sphere-on-rod structure can be estimated according to Blevins [11] as:

$$\omega_0 = \sqrt{\frac{3EI}{L^3(m_{sph} + 0.24m_r)}} \tag{2}$$

where ω_0 is the fundamental angular resonance frequency, L is the length of the rod, m_r is the mass of the rod, E is its Young's modulus and I its area moment of inertia, and m_{sph} is the mass of the sphere. Considering the fundamental vibration of the sphere-on-rod as a single-degree-of-freedom dynamic system, it can be described by the equation

$$m(-\omega^2 + i\omega_0\omega/Q + \omega_0^2)u = F \tag{3}$$

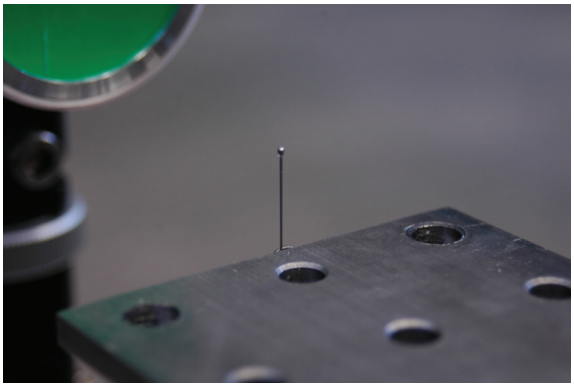

Figure 1. Sphere on rod.

where u is the structural displacement of the sphere, F is the force acting on the sphere, ω is the angular frequency, ω_0 is the angular resonance frequency, Q is the quality factor of the resonance and m is the effective mass. From Eq. 2 it can be seen that the effective mass m is equal to

$$m = m_{sph} + 0.24m_r \tag{4}$$

At resonance $\omega = \omega_0$, and Eq. 3 simplifies into:

$$mi\omega_0^2 u/Q = F \tag{5}$$

or, if the response is measured as a velocity v:

$$F = m\omega_0 v/Q \tag{6}$$

In the following section the practical aspects of the test set-up are discussed and the measurement results are shown. In addition the model derived in this section is validated by comparing the model results with the experimental results. Finally, based on the validated model the acoustic radiation forces are estimated.

4. Experiments

4.1. Ultrasonic transducer and laser vibrometer

In the experimental test set-up a point focussed ultrasonic transducer from Ultran is used (see www.ultrangroup.com), type NCG200-D38-P50, with a nominal operation frequency of 200 kHz and a focal distance of 50 mm. These transducers employ novel acoustic impedance matching layers to overcome the big difference in acoustic impedance of a PCT-based transducer and air. In addition these transducers are manufactured from high coupling piezoelectric materials [12]. This results in an ultrasonic actuator that radiates acoustic noise in air very efficiently. The sphere-on-rod resonant structure is brought into vibration by means of the acoustic radiation forces

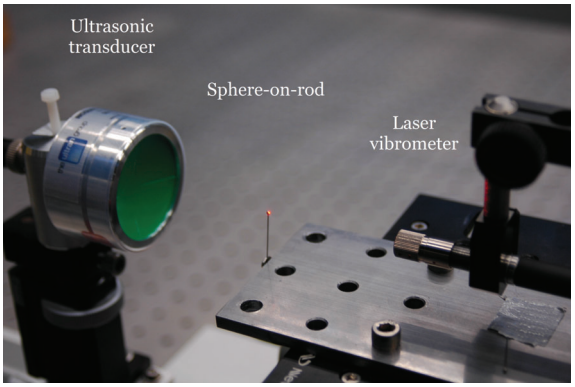

Figure 2. Sphere on rod with laser.

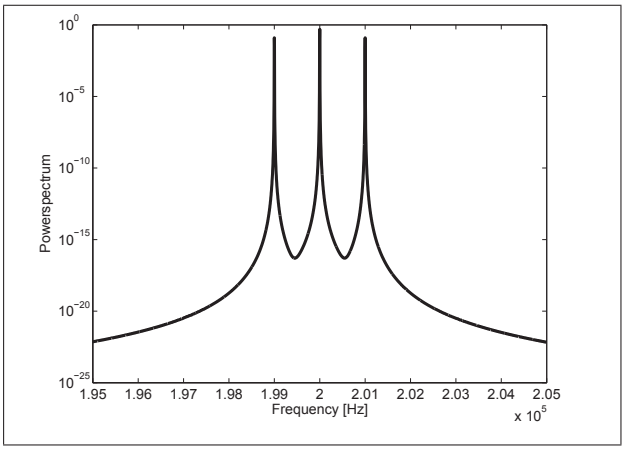

Figure 3. Spectrum of a synthesized AM modulated signal, f_c=200kHz, f_{AM}=1kHz.

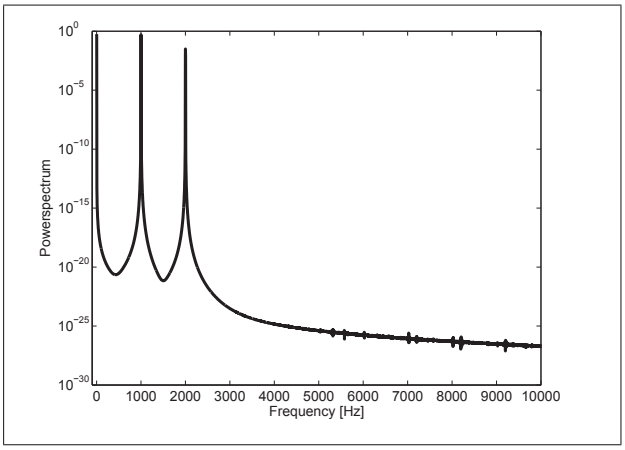

Figure 4. Spectrum of the synthesized AM modulated signal squared, lower frequency range only.

resulting from the ultrasonic waves of the focused transducer. The sphere is located in the focal point of the transducer as good as possible. This focal point is found manually by maximizing the structural response of the sphere-on-rod resonant structure for different positions of the sphere relative to the transducer.

The vibrations of the sphere-on-rod resonant structure are measured by means of a Polytec laser-vibro meter system, comprising an OFV552 fiber vibrometer and an OFV5000 vibrometer controller with a VD-09 decoder. This decoder is capable of measuring up to 100kHz with a high sensitivity of 5 mm/s/V. In practice a relatively high optical reflection on the steel sphere could be obtained, resulting in a high quality laser-vibrometer signal. Figure 2 shows the test set-up.

4.2. Two-sine and AM modulation

To create a dynamic acoustic radiation force, Fatemi and Greenleaf [3] employed two superimposed ultrasonic acoustic waves of slightly different frequencies ω_1 and ω_2, with $\omega_2 > \omega_1$. Because of the non-linear behaviour of the acoustic radiation force, an acoustic radiation force will be created at the difference frequency $\omega_2 - \omega_1$. This low frequency component $\omega_2 - \omega_1$ can be exploited to excite a structure dynamically.

Alternatively, an AM-modulated ultrasonic signal can also be used to generate low-frequency radiation force components. AM-modulated signals consist of three frequency components, i.e. the carrier frequency, f_c, the carrier frequency increased with the AM-modulation frequency, $f_u = f_c + f_{AM}$, and the carrier frequency minus the AM-modulation frequency, $f_l = f_c - f_{AM}$. In Fig. 3 the spectrum of a synthesized AM-modulated signal is shown. Because the acoustic radiation force scales quadratically with the acoustic pressure, the spectrum of the acoustic radiation force will contain not only the ultrasonic components f_c, f_l and f_u, but also sum and difference frequency terms. In the sonic frequency range, this will give rise to the difference frequencies $f_c - f_l = f_{AM}$ and $f_u - f_l = 2f_{AM}$. Figure 4 shows the spectrum of the synthesized signal squared, for the lower frequencies only, to illustrate this effect. We preferred the AM-modulation approach above the two-sine approach because standard measurement equipment with AM-modulation is readily available.

In the experiments a Philips PM5193 0.1 mHz to 50 MHz synthesized function generator was employed. To verify the signal generated by the Philips PM5193 it was analysed by means of a HP4396 Network/spectrum analyzer. The measurements were carried out for a carrier frequency of 200kHz and an AM modulation frequency of 1kHz. Maximum AM-modulation was attained, as shown in Fig. 5 (channel 1 is the AM-modulation, channel 2 is the AM-modulated signal). The spectrum of the AM-modulated signal, as analysed by the HP4396 is shown in Fig. 6. From this figure it can be seen that three frequency components dominate the signal, at 200 kHz, which is the carrier frequency, and at 199kHz and 201kHz, as expected. The suppression of harmonic frequencies is better than 50 dB.

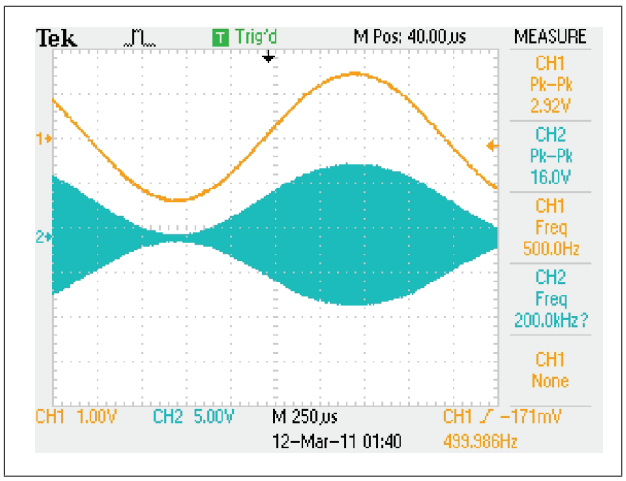

Figure 5. Time signals of a 500 Hz AM-modulation signal (top curve) and the AM-modulated signal with a carrier frequency of 200kHz (bottom curve).

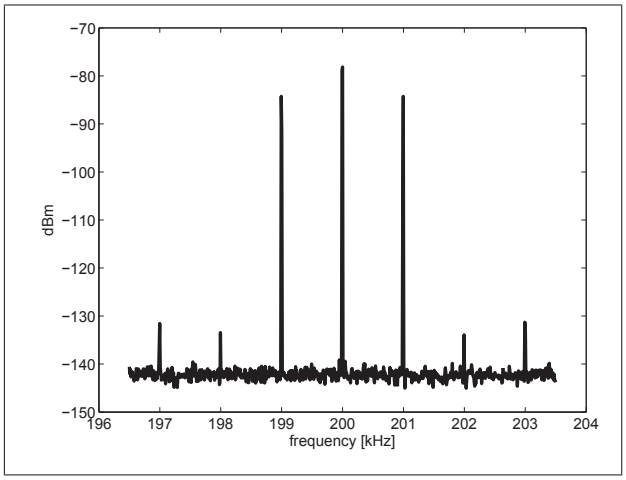

Figure 6. Spectrum of the AM-modulated signal as generated by the Philips PM5193 (f_c=100kHz, f_{AM}=1kHz, $20V_{pp}$).

4.3. Sphere-on-rod measurement results

In the measurements the frequency response functions from AM-modulation signal to structural velocity of the sphere were measured, i.e.

$$H(\omega) = \frac{v(\omega)}{V(\omega)}. \tag{7}$$

Where $V(\omega)$ is the modulation depth, expressed in Volts. A voltage of 1.4 V means 100% modulation for the Philips PM5193 synthesized function generator. The units of the frequency response functions are thus [m/s/V]. Note that when employing AM-modulation with a modulation frequency ω, acoustic radiation forces will be generated at both ω and 2ω (cf. Fig. 4). To estimate a well-defined frequency response function, the measurements were performed with a swept sine excitation combined with a FFT-zoom technique, in which the frequency range was chosen such that we

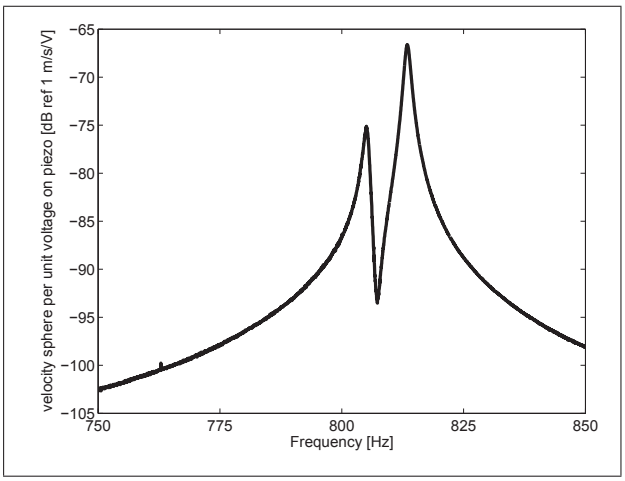

Figure 7. Typical frequency response function (sphere on rod 1mm)

are only dealing with a force due to the ω component. In practice this means for instance that for a sphere-rod resonance frequency of approximately 800 Hz, the frequency sweep was performed from 750 Hz up to 850 Hz, using a frequency step of 0.03125 Hz (3201 frequency lines). The FFT-zoom measurements were also confined to this frequency region. In this manner, the 2ω frequency component falls outside the frequency range which is considered by the measurements. A typical frequency response function is shown in Fig. 7.

The double peak in Fig. 7 is caused by two eigenmodes of the sphere-on-rod, in two orthogonal directions, having closely spaced resonance frequencies. Due to geometrical differences in the clamping of the rod the two resonance frequencies are not exactly the same. The mode which vibrates predominantly in the direction of the laser-beam and ultrasonic transducer is measured at a higher vibration level as compared to the mode which is predominantly vibration in perpendicular direction. In an additional experiment the sphere-on-rod was rotated 90 degrees, to demonstrate that the level of excitation and measurement of the two modes are interchanged, as shown Fig. 8.

Varying the voltage of the carrier signal, remaining maximum AM-modulation in all cases, we can see that the amplitude of the frequency response function defined in Eq. 7 changes quadratically with carrier voltage as can be seen in Fig. 9. Figure 10 zooms in on the resonance peaks. At a carrier voltage of 20V peak-peak the response peak measures about -66.5 dB re 1m/s/V, and at a carrier voltage of 10V peak-peak it measures about -78.5 dB re 1m/s/V, which is precisely 12 dB lower. This indeed verifies that the radiation force is proportional to the acoustic pressure squared, as shown in Eq. 1.

Table I. Measurement results sphere-on-rod experiments.

Sphere radius [mm]		0.5	0.75	1	1.25	1.5
Sphere mass [mg]		8.3	19.1	37.4	68.9	115.7
Resonance frequency ($\omega_0/2/\pi$) [Hz],	series 1	860.6	554.0	357.2	303.7	231.6
	series 2	766.3	555.8	445.8	288.5	230.6
	series 3	957.0	580.4	421.3	298.3	231.0
On-resonance velocity $v(\omega_0)$ [dB re. 1 m/s],	series 1	-61.6	-63.4	-61.0	-66.2	-65.0
	series 2	-62.6	-66.9	-68.3	-62.3	-64.9
	series 3	-64.1	-63.4	-72.0	-64.0	-65.2
Q-factor [-]	series 1	642	593	543	456	432
	series 2	409	399	379	482	410
	series 3	447	566	156	449	316
Estimated radiation force [μN]	series 1	0.082	0.089	0.150	0.148	0.223
	series 2	0.102	0.089	0.115	0.206	0.237
	series 3	0.098	0.097	0.174	0.188	0.298

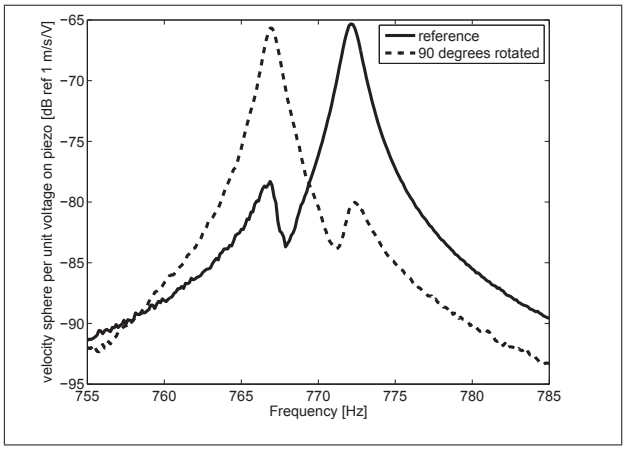

Figure 8. Frequency response function of a sphere on rod excited at 0 degrees and at 90 degrees.

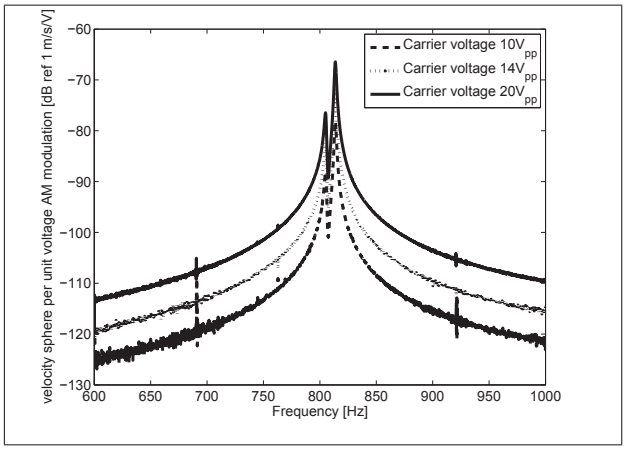

Figure 9. Effect of changing carrier voltage on the frequency response function.

4.4. Model validation

The measurement results were fitted by means of the one-dimensional sphere-on-rod model as derived in Section 3, to obtain estimates for the angular resonance frequency, ω_0, the maximum velocity amplitude at resonance, $v(\omega_0)$, and the quality factor Q.

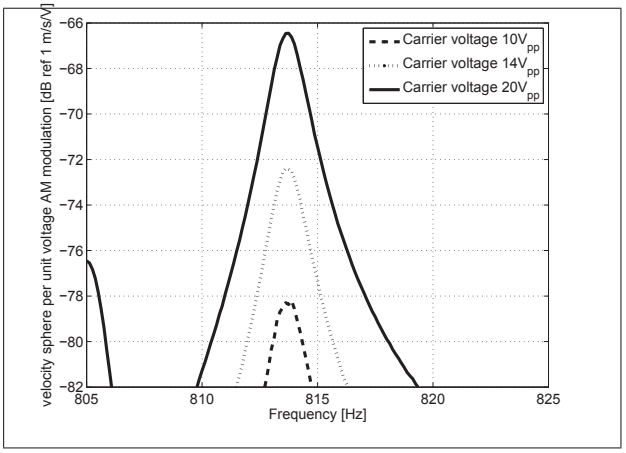

Figure 10. Effect of changing carrier voltage on the frequency response function, zoomed in on resonance peaks.

The weight of each sphere-on-rod mechanical system, with the sphere glued on the rod, was measured by a balance with an accuracy of 0.1 mg. The weight of the sphere, including the glue, was calculated by subtracting the measured weight of the individual rods without sphere glued on it. Furthermore, additional measurements in the time-domain were carried out to estimate the quality factor Q more accurately.

As an example, the frequency response function of a fitted model was plotted together with the directly measured frequency response function in Fig. 11. It can be seen that the main resonance peak is fitted very well with the one-dimensional model.

4.5. Acoustic radiation force estimations

Three series of measurements were performed on a number of sphere-on-rod resonators with varying sphere diameters. The rods all have a radius of 0.2 mm and a length of approximately 15 mm. The spheres that were used in the experiments have a radius of 0.5 mm, 0.75 mm, 1 mm and 1.5 mm, respectively. The spheres are glued to the end of a rod as shown in Fig. 1. For each measurement series the sphere-on-rods were dismounted and remounted on a rigid

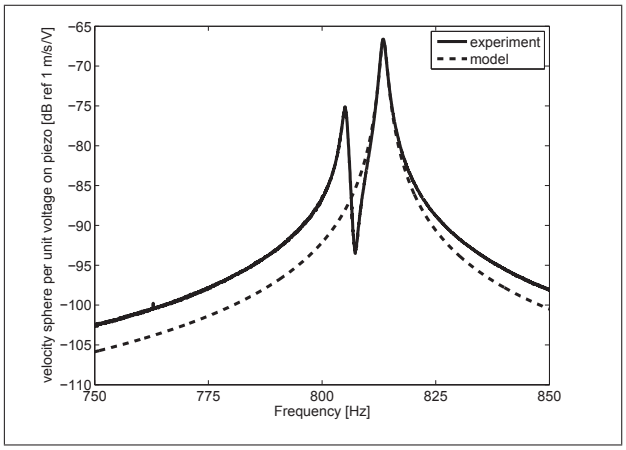

Figure 11. Model versus measurements for a typical frequency response function (sphere on rod 1mm).

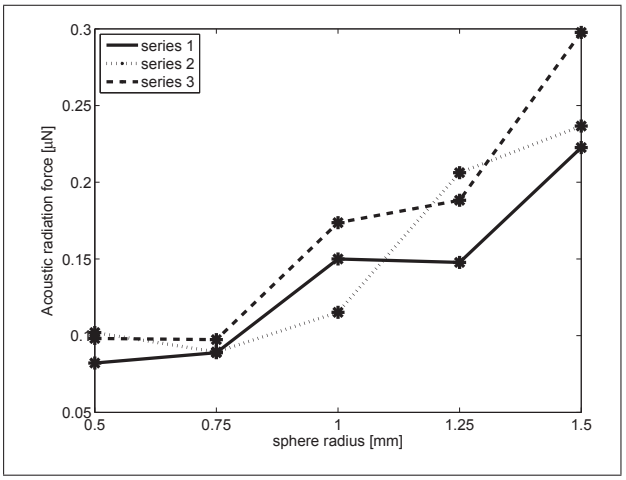

Figure 12. Radiation force estimates.

base. During remounting it was not possible to retain exactly the same rod-length, resulting in different eigenfrequencies. Because of the remounting, different clamping conditions will occur, resulting in different Q-factors as well. This is not a serious problem, since the measured eigenfrequencies and Q-factors of the sphere-on-rod mechanical systems are used for the computation of the acoustic radiation force according to Eq. 6. The results of these measurements are given in Table I, together with the estimated acoustic radiation force. During the measurements the velocity frequency response function $H(\omega_0)$, as defined in Eq. 7, is measured. Knowing that maximum AM-modulation occurs for a modulation depth voltage V=1.4 Volt, the peak velocity for maximum AM-modulation at the structural resonance, $v(\omega_0)$, can be determined easily. This maximum is given in the table, as well as the corresponding acoustic radiation force. The AM-modulated carrier has a peak-peak voltage of 16 Volt, beging generated by the Philips PM5193 synthesized function generator (see Fig. 5).

The estimated acoustic radiation force is graphically presented as function of the sphere radius in Fig. 12. From this figure it can be seen that the acoustic radiation force increases with increasing sphere radius. Because the sphere radii considered are much larger compared to the acoustic wavelength, the cube power dependency as suggested by Eq. 1 is not applicable. Note that Eq. 1 is valid for $ka < 0.14$, whilst in the conducted experiment for the smallest sphere radius $ka = a\omega/c$=0.5e-3*2*pi*200e3/340 = 1.8. In fact, curve fitting the measured acoustic radiation forces F as function of sphere radius r with a function of the type $F = ar^b$, yields a value for b of only 1.4.

5. CONCLUSIONS

Experiments on resonant structures, consisting of spheres that are glued on a rod, reveal that the dynamic acoustic radiation force magnitude is approximately 0.1 μN and 0.25 μN for a sphere with a diameter of 1mm and 3mm, respectively, driving the ultrasonic transducer at 200kHz, AM-modulated, at 10 Volts peak. It is also shown that the acoustic radiation force scales with the sphere diameter to the power 1.4 and scales quadratically with the transducer voltage. The measurements were carried out with a point focussed ultrasonic transducer with a diameter of 38 mm and a focal length of about 50 mm.

Acknowledgement

This work has been supported by AgentschapNL, under contract number Point One PHEH10007. We gratefully acknowledge Mahesh C. Bhardwaj of the Ultran group, PA, USA, www.ultrangroup.com, for making ultrasonic transducers available. We also greatly acknowledge Prof. Andreas Dietzel, affiliated to Holst Centre, Eindhoven and the Eindhoven University of Technology, the Netherlands and Prof. Henk Nijmeijer for the use of the laboratories.

References

[1] Lord Rayleigh, On the pressure of vibration, Philos. Mag. 3, 338 (1902)

[2] Chu and Apfel, Acoustic radiation pressure produced by a beam of sound, J. Acoust. Soc. Am. 72 (1982).

[3] Fatemi and Greenleaf, Ultrasound-Stimulated Vibro-Acoustic Spectrography, Science 280, 82 (1998).

[4] Alizad, Whaley, Greenleaf and Fatemi, Critical issues in breast imaging by vibro-acoustography, Ultrasonics Vol. 44(1), 217-220 (2006)

[5] Huber, Purdham, Fatemi, Kinnick, and Greenleaf, Non-contact mode excitation of small structures in air using ultrasound radiation force, J. Acoust. Soc. Am. 117(4), April 2005

[6] Huber, Ofstad, Barthell, Raman, Spletzer, Excitation of Vibrational Eigenstates of Coupled Microcantilevers, Proceedings of the ASME 2008 International Design Engineering Technical Conferences & Computers and Information in Engineering Conference IDETC/CIE 2008, August 3-6, 2008, Brooklyn, New York, USA

[7] Huber, Fatemi, Kinnick, and Greenleaf, Noncontact modal analysis of a pipe organ reed using airborne ultrasound stimulated vibrometry, J. Acoust. Soc. Am. 119 (4), April 2006

[8] King, Proc. R. Soc. London, Ser. A 147, 212 (1934)

[9] Lee and Feng, Acoustic levitating apparatus for submillimeter samples,Rev. Sci. Instrum. 53(6), 854-859 (1982)

[10] Vandaele, Contactless handling for micro-assembly: acoustic levitation, PhD thesis Université libre de Bruxelles (2008)

[11] Blevins, Formulas for natural frequency and mode shape, Von Nostrand Reinhold Company, 1979

[12] Bhardwaj, Phenomenally high transduction air-gas transducers for practical non-contact ultrasonic applications, AIP Conference Proceedings 2009, in : Review of Quantitative Nondestructive Evaluation Vol. 28, American Institute of Physics, 2009